# Luminescent Homoatomic Exciplexes in Dicyanoargentate(I) Ions Doped in Alkali Halide Crystals. 2. "Exciplex Tuning" by Varying the Dopant Concentration[†]

**Mohammad A. Omary,[‡,||] Derek R. Hall,[§,⊥] George E. Shankle,[§] Aleksander Siemiarczuk,[∇] and Howard H. Patterson*[,‡]**

*Department of Chemistry, University of Maine, Orono, Maine 04469, Department of Chemistry, Angelo State University, San Angelo, Texas 76909, and Fast Kinetics Application Laboratory, Photon Technology International, 347 Consortium Court, London, Ontario N6E 2S8, Canada*

*Received: January 5, 1999; In Final Form: March 16, 1999*

The dependence of the dicyanoargentate(I) luminescence on the dopant concentration in $[Ag(CN)_2^-]$/KCl single crystals is reported. Three crystals with different Ag content have been studied. The photoluminescence spectrum of the doped crystal that has the lowest silver content (0.17%) is dominated by a high-energy band at ~295 nm, while the spectrum with the highest silver content (4.3%) is dominated by a low-energy luminescence band at ~400 nm. The crystal with an intermediate Ag content (2.7%) shows strong emissions from both the high-energy and low-energy bands. Time-resolved luminescence measurements indicate that the excitation energy is transferred between different $[Ag(CN)_2^-]_n$ oligomers and, thus, leads to the tunable emission observed in the $[Ag(CN)_2^-]$/KCl system. The mechanisms of the radiative and nonradiative processes have been described by a kinetic model that describes the experimental lifetime and time-resolved data.

## Introduction

The use of inorganic materials in technological applications has been growing in recent years. Many inorganic materials have demonstrated potential use as photocatalysts,[1] environmental sensors,[2] solar energy converters,[3] nonlinear optical devices,[4] laser materials and phosphors,[5] semiconductors and superconductors,[6] and photoluminescent probes of biological systems.[7] Among the materials that have shown potential in the aforementioned applications have been coordination compounds of group 11 monovalent ions. For example, some Cu(I) coordination compounds have been used to photosensitize water splitting via energy- and electron-transfer pathways.[8] Other reports have suggested the potential use of Cu(I) in tunable solid-state materials in the UV.[9,10] Gold(I) compounds have been suggested for applications such as biosensors,[11] photocatalysts,[12] and optical sensors for volatile organic compounds.[13]

Most of the attention given to silver(I) compounds has been concentrated on photophysical and photochemical studies of simple silver halides[14−16] due to the various applications of these compounds. Besides the well-known applications in photographic materials, silver halides have been also used for optical fibers, especially in the mid-IR region.[17] A series of studies by Pedrini has addressed the photophysical properties of Ag(I) ions doped in alkali halides.[18] More recently, luminescence studies of different Ag(I) centers have been reported in glassy and crystalline borate[19] and in phosphate glasses.[20] Interest in silver(I) oxides has been stimulated by their use as conductors, semiconductors, and photoconductors.[6,21−23]

Despite the tremendous attention given to Ag(I) halides, oxides, and doped ions in the literature, very little work has been reported to address the photophysics and photochemistry of Ag(I) coordination compounds.[24−27] We have recently studied Ag(I) coordination compounds to elucidate fundamental issues in chemistry such as ligand-unsupported Ag−Ag closed-shell interactions (argentophilic attraction)[28] and inorganic excimers and exciplexes.[29] We have started an investigation of $[Ag(CN)_2^-]$ doped in alkali halide hosts. Single crystals of these systems have demonstrated remarkably rich photoluminescence properties, as manifested by a new optical phenomenon we called "exciplex tuning".[30] In part 1 of this series, we have studied exciplex tuning by site-selective spectroscopy, in which the luminescence can be tuned to several bands in the 285−610-nm range simply by varying the excitation wavelength in a single $[Ag(CN)_2^-]$/KCl doped crystal.[30] The tunability of the emission energy in the $[Ag(CN)_2^-]$/KCl system compares favorably with other systems that have been reported to display efficient tuning of their excited states. For example, Yersin and Gliemann have described the tunability of the luminescence energy in the tetracyanoplatinates(II).[31] However, to tune the emission over a long energy range, a combination of chemical substitution (changing the counterion) and application of high pressure must be applied to $[Pt(CN)_4]^{2-}$ systems. More recently, Cummings and Eisenberg have reported efficient tuning of the charge-transfer absorption and emission of Pt(diimine)(dithiolate) by 8160 and 7400 $cm^{-1}$, respectively.[32] Thirteen complexes were synthesized by varying the ligands in order to achieve this efficient tuning in the visible range. In exciplex tuning, on the other hand, the emission can be tuned by more than 18 000 $cm^{-1}$ in the UV and visible range in a single crystal of $[Ag(CN)_2^-]$/KCl, simply by changing the excitation wavelength. This result is promising toward potential applications based on dicyanoargentate(I) systems.

We report herein exciplex tuning by varying the dopant concentration. Variation of the doping level of $[Ag(CN)_2^-]$ in

---

[†] For part 1, see: Omary, M. A.; Patterson, H. H. *J. Am. Chem. Soc.* **1998**, *120*, 7696.

[‡] University of Maine.

[§] Angelo State University.

[∇] Photon Technology International.

[||] Present address: Department of Chemistry, Colby College, Waterville, ME 04901.

[⊥] Present address: Department of Chemistry, University of Texas at Austin, Austin, TX 78712.

10.1021/jp990060v CCC: $18.00

**TABLE 1: Parameters Used in Extended Hückel Calculations[a,b]**

| atom | orbital | $H_{ii}$ (eV) | $\xi$ | interatomic distance, Å |
|---|---|---|---|---|
| Ag | 4d | −13.91 | 3.248 | Ag−C, 2.08 |
| | 5s | −6.453 | 1.594 | C−N, 1.09 |
| | 5p | −3.289 | 1.170 | |
| C | 2s | −19.39 | 1.577 | |
| | 2p | −11.07 | 1.434 | |
| N | 2s | −26.25 | 1.886 | |
| | 2p | −13.83 | 1.728 | |

[a] Orbital energies and wave functions are taken from ref 34. [b] Average interatomic distances in Tl[Ag(CN)$_2$] (ref 28).

the host KCl crystal leads to a change in the relative intensities of the luminescence bands. A correlation is sought between the Ag content in the mixed crystals and the identity of the major luminescent exciplex. A kinetic model is presented to explain the energy-transfer pathways between various emitting centers in the mixed crystals.

## Experimental Section

Crystals were grown by slowly evaporating at ambient temperature aqueous solutions containing approximately 2 M KCl and 0.05 M KAg(CN)$_2$. By harvesting samples at different stages during the evaporation, doped crystals of KCl with different [Ag(CN)$_2^-$] contents were obtained. The silver content was determined by atomic absorption spectroscopy using a Varian SpectrAA-20 spectrophotometer with an air−acetylene flame and a Ag analytical lamp operating at 328.1 nm. The standards for the atomic absorption analysis were prepared using Aldrich 1000 ppm Ag standard in 1% HNO$_3$. Atomic absorption measurements were run in triplicate for each sample of crystals harvested at the same time, for which the results showed no variability of the Ag content (to two significant figures).

Steady-state photoluminescence spectra were recorded with a model QuantaMaster-1046 fluorescence spectrophotometer from Photon Technology International, PTI. The instrument is equipped with two excitation monochromators and a 75-W xenon lamp. The excitation spectra were corrected for the lamp background following the standard quantum counter method by dividing the raw data by the excitation spectrum of rhodamine B ($\lambda_{em} = 635$ nm).[33] Lifetime and time-resolved measurements were carried out with a LaserStrobe system from PTI equipped with a nitrogen laser, a dye laser, a frequency doubler, and a gated microsecond detector for the microsecond time domain. Some measurements were also carried out with a QuantaMaster-2 system utilizing a microsecond Xe flash lamp and a gated microsecond detector. All luminescence spectra were recorded at liquid nitrogen temperature for single crystals using either a model LT-3-110 Heli-Tran cryogenic liquid-transfer system or a supracell quartz capillary tube inserted into a liquid nitrogen Dewar flask with a quartz window.

Fourier transform infrared (FTIR) spectra were obtained using a Bio-Rad Digilab FTS-60 spectrometer equipped with a microscope accessory and a liquid nitrogen-cooled detector. This setup allows for measuring the FTIR spectra of single crystals using the reflectance mode. The crystal was mounted on a gold-plated metal plate, which serves as a reference for the reflectance spectra, and aligned visually using the microscope prior to the acquisition of the infrared spectra.

**Computational Details.** Ground- and excited-state extended Hückel calculations were carried out using the FORTICON8 program (QCMP011). Table 1 summarizes the interatomic distances and the relativistic parameters used in the calculations.[28,34] Potential surfaces for both the ground state and the first excited state were generated for geometrical isomers of isolated dimer and trimer units of [Ag(CN)$_2^-$].

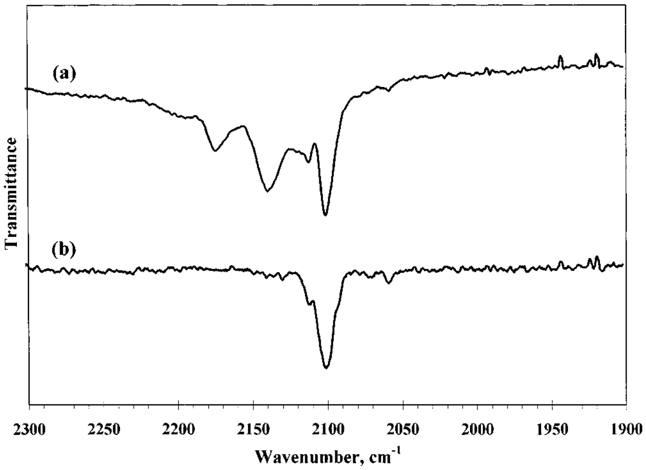

**Figure 1.** Infrared spectra of single crystals of [Ag(CN)$_2^-$]/KCl in the region of the cyanide stretching frequency. The spectra are shown for single crystals with % Ag of 4.3 (a) and 0.17 (b), denoted in the text as P3 and P1, respectively.

## Results and Discussion

**Atomic Absorption and FTIR Data.** Three harvests (P1, P2, and P3) of [Ag(CN)$_2^-$]/KCl mixed crystals have been studied. The three harvests have been isolated from the same batch but at different times during the slow evaporation. Atomic absorption analysis has shown that the values of % Ag (by wt) are 0.17, 2.7, and 4.3 for P1, P2, and P3, respectively. The difference in the silver content between the different harvests is explained as follows: The saturated KCl solution contains impurities of [Ag(CN)$_2^-$] ions. Therefore, as the solution evaporates, the crystals harvested in the early stages of the slow evaporation are predominantly KCl crystals with a very low concentration of [Ag(CN)$_2^-$]. After these crystals have been removed, the concentration of [Ag(CN)$_2^-$] in the mother liquor increases, and therefore the next harvest isolated will have a higher silver content.

The infrared spectra of the three crystals studied show multiple peaks in the $\nu_{C-N}$ region. Figure 1a shows the infrared spectrum of P3. Four well-resolved peaks at ~2100, 2110, 2140, and 2175 cm$^{-1}$ are distinguished in Figure 1a. This result indicates the presence of several environments of [Ag(CN)$_2^-$] ions in the mixed crystal. Previous data for M[Ag(CN)$_2$] pure crystals support this argument. For example, infrared spectra for solid K[Ag(CN)$_2$] have been reported previously and show only one strong, unstructured band in the $\nu_{C-N}$ region.[35a,b] This band appears at 2140 cm$^{-1}$ and is assigned to the $\upsilon_3$ fundamental mode (C−N asymmetric stretch) of the $D_{\infty h}$ [Ag(CN)$_2^-$] ion. Raman spectra of crystalline K[Ag(CN)$_2$] also show only one unstructured $\nu_{C-N}$ band.[35c,d] This band appears at ~2148 cm$^{-1}$ and is assigned to the $\upsilon_1$ fundamental mode (C−N symmetric stretch) of the $D_{\infty h}$ [Ag(CN)$_2^-$] ion. Single crystals of K[Ag(CN)$_2$], from which the mixed crystals reported herein were prepared, also yielded a single unstructured band in the $\nu_{C-N}$ region.[36] These data are consistent with the crystal structure of K[Ag(CN)$_2$] which indicates the presence of only one unique Ag site.[37] In contrast, both FTIR and Raman spectra of a single crystal of Tl[Ag(CN)$_2$] show multiplets in the $\nu_{C-N}$ region. This pattern has been correlated with the crystal structure of Tl[Ag(CN)$_2$] which shows three crystallographically distinct Ag sites.[28] The different sites of [Ag(CN)$_2^-$] ions in the KCl lattice

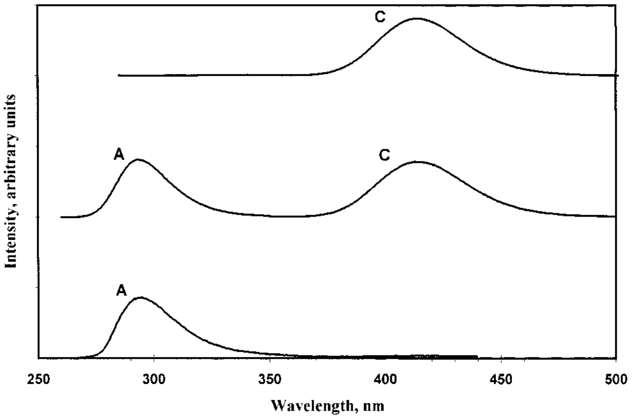

**Figure 2.** Exciplex tuning by varying the dopant concentration: emission spectra of $[Ag(CN)_2^-]$/KCl crystals at 77 K. The spectra are shown for crystals with a silver content of (bottom to top): 0.17 (P1), 2.7 (P2), and 4.3% (P3). Each sample was excited with wavelengths that correspond to its most prominent excitation band(s) (see Table 2). The spectrum shown for P2 is a composite of two spectra with excitations corresponding to both bands A and C. The intensities are comparable in this composite spectrum. The relative intensities are not comparable between spectra of different crystals.

are, therefore, explained by the presence of these ions in different environments and therefore different site symmetries. This is due to impurity sites in the KCl host crystal created by the doped $[Ag(CN)_2^-]$ ions that are present in different aggregations, i.e., $[Ag(CN)_2^-]_n$. The FTIR setup was sensitive even to the crystal with the lowest concentration of $[Ag(CN)_2^-]$ (i.e., P1). The infrared spectrum of P1 shows a major peak at $\sim$2100 cm$^{-1}$ with two shoulders at $\sim$2090 and 2110 cm$^{-1}$ (Figure 1b). This suggests that multiple C−N sites are present even in the crystal with a small silver content (0.17%), albeit to a lower extent than in crystals with higher % Ag. The observation of peaks at high frequencies in the infrared spectrum of the crystal with high silver content (P3) is attributed to the increase in the number of sites with a higher aggregation of $[Ag(CN)_2^-]$ units. This means that silver−silver interactions increase; thus, the electron density provided by silver to the cyanide ligands decreases. Since the LUMOs of $CN^-$ are antibonding ($\pi^*$), the decreasing electron density from silver leads to stronger C−N bonds and, consequently, higher $\nu_{C-N}$. It should be noted that by virtue of the microscope setup of our FTIR spectrometer, the infrared spectra shown in Figure 1 are for the same intact single crystals used for the optical studies in this work, which allows good correlation with the photoluminescence spectra.

**Steady-State Photoluminescence Spectra.** Figure 2 shows the steady-state photoluminescence spectra of P1, P2, and P3 at 77 K. According to Figure 2, a high-energy band (A) predominates the luminescence spectra of the mixed crystal with the lowest Ag content, P1 (bottom spectrum). On the other hand, a low-energy band (C) predominates the luminescence spectra of the crystal with the highest Ag content, P3 (top spectrum). Interestingly, the crystal with an intermediate silver content, P2, shows emissions of both bands A and C with rather similar intensities.

The assignment of the luminescence bands of $[Ag(CN)_2^-]$/KCl systems is summarized in Table 2.[30] Although all four bands have been observed in all three crystals, the discussion herein is restricted to bands A and C. The relative intensity of band D in the emission spectra of all three crystals is too weak for conclusions to be drawn. Also, the appearance of band D is more influenced by other factors than the doping level. These factors, which include the irradiation history of the crystal, will be reported in due course. On the other hand, both bands B and C are assigned to $[Ag(CN)_2^-]_3$ trimers, and we have chosen to discuss the concentration dependence of the lower-energy band characteristic of the trimer (band C). Band B is not included in the analysis herein due to the strong overlap between bands B and C.[30] This overlap between bands B and C is further characterized by our time-resolved measurements (vide infra).

In Table 2, all the luminescence bands are assigned to oligomers of the $[Ag(CN)_2^-]$ complex. The presence of other complexes such as $[Ag(Cl)_2^-]$ or $[Ag(Cl)(CN)^-]$ is ruled out based on the much higher formation constant for $[Ag(CN)_2^-]$. The overall formation constant of $[Ag(CN)_2^-]$ is $10^{20}$ M$^{-2}$.[38a] This value is more than $10^{13}$ times greater than that for $[Ag(Cl)_2^-]$.[38b] Therefore, the dicyano complex is expected to be the dominant species present in the KCl doped crystals in this study. Moreover, the luminescence bands displayed by the doped KCl crystals correlate with those displayed by pure crystals of $M[Ag(CN)_2]$ (for example, with M = $Tl^+$, $K^+$, $Cs^+$, $Rb^+$, $Ca^{2+}$, $Sr^{2+}$).[36] Since these pure crystals do not contain any chloride ions and show the same luminescence bands as those shown by the doped crystals discussed herein, we rule out the contribution of chloride-containing complexes in the doped crystals.

The relative intensities in Figure 2 can be explained based on the different extent of Ag−Ag interactions in the three crystals. The probability of $[Ag(CN)_2^-]_n$ oligomers with large "*n*" values in the $[Ag(CN)_2^-]$/KCl system increases on going from crystals with low $[Ag(CN)_2^-]$ concentrations in KCl to those with higher concentrations. Therefore, the crystal with only 0.17% Ag contains mostly isolated ions or dimers of $[Ag(CN)_2^-]$. Since isolated ions are not emissive,[30] the observed luminescence is attributed to $*[Ag(CN)_2^-]_2$; thus, only the excimer emission is strong in P1. The fact that the infrared spectrum of P1 only shows a smaller number of bands in the $\nu_{C-N}$ region, all of which are at low frequencies, is consistent with this assignment. Meanwhile, P3 has a much higher silver content (more than 25 times higher % Ag than P1). Consequently, a higher probability exists for finding trimers and longer-chain oligomers in P3 than in either P1 or P2. Emissions due to localized exciplexes are, therefore, expected to be more important in P3. The infrared spectrum of P3 also supports this argument as evidenced by the presence of a number of bands at high frequencies (Figure 1a).

**Statistical Distribution Analysis.** In an attempt to relate the relative intensities of bands A and C to the Ag content in the $[Ag(CN)_2^-]$/KCl system, we have carried out a statistical distribution analysis for the relative population of $[Ag(CN)_2^-]_n$ oligomers ($n = 1-3$) in the face-centered cubic KCl lattice. The $[Ag(CN)_2^-]$ monomer has one possible isomer in the KCl lattice. The monomer population is calculated as the ratio of the number of Ag sites relative to the total cation sites in the KCl lattice. This ratio is equal to the mol % of Ag in a given doped crystal. Therefore, the total monomer population ($p$) is 0.12, 1.9, and 3.0% in the three crystals studied (P1, P2, and P3, respectively). The statistical distribution analysis for the monomer and the different geometrical isomers of the $[Ag(CN)_2^-]_2$ dimer and the $[Ag(CN)_2^-]_3$ trimer in the three crystals studied are shown in Table 3. The description of the calculation method is illustrated herein for the $[Ag(CN)_2^-]_2$ dimer and can be followed using a model for a KCl (or NaCl) lattice.

The orientation of the $[Ag(CN)_2^-]$ linear units in the KCl lattice is important in the calculations of the statistical distribution analysis. Chart 1 shows the orientation of one isomer of $[Ag(CN)_2^-]_2$ in KCl. The $[Ag(CN)_2^-]_2$ dimer has three isomers

**TABLE 2: Assignment of the Luminescence Bands of [Ag(CN)$_2^-$]/KCl Crystals**

| band | $\lambda_{max}^{em}$, nm | $\lambda_{max}^{exc}$, nm | fwhm, $10^3$ cm$^{-1}$ | assignment |
|---|---|---|---|---|
| A | 285−300 | 225−250 | 3.31 | *[Ag(CN)$_2^-$]$_2$ (excimers) |
| B-1[a,b] | 310−330 | 270−290 | 3.70 | *[Ag(CN)$_2^-$]$_3$ (localized exciplexes)[a] |
| B-2[a,b] | 340−360 | 270−290 | 3.70 | *[Ag(CN)$_2^-$]$_3$ (localized exciplexes)[a] |
| C[a] | 390−430 | 250−270 | 3.05 | *[Ag(CN)$_2^-$]$_3$ (localized exciplexes)[a] |
| D | 490−530 | 300−360 | 4.01 | *[Ag(CN)$_2^-$]$_n$ (delocalized exciplexes) |

[a] Bands B-1, B-2, and C represent three different geometrical isomers of [Ag(CN)$_2^-$]$_3$ trimer (see Chart 2). [b] Bands B-1 and B-2 were labeled as one band (B) in ref 30. The fwhm value herein refers to the band width of bands B-1 and B-2 combined.

**TABLE 3: Statistical Distribution Analysis of the Geometrical Isomers of the [Ag(CN)$_2^-$]$_2$ Dimer and the [Ag(CN)$_2^-$]$_3$ Trimer in the Three [Ag(CN)$_2^-$]/KCl Crystals Studied: P1, P2, and P3**

| | | Ag, mol % | | | relative probability[b] | | |
|---|---|---|---|---|---|---|---|
| species[a] | probability | P1 | P2 | P3 | P1 | P2 | P3 |
| monomer | $p$ | 0.12 | 1.9 | 3.0 | 100 | 100 | 100 |
| total dimer | $12p^2$ | 0.0016 | 0.41 | 1.0 | 0.23 | 15 | 24 |
| D1 | $(20/3)p^2$ | 0.00091 | 0.23 | 0.58 | 0.13 | 8.5 | 14 |
| D2 | $(4/3)p^2$ | 0.00018 | 0.046 | 0.12 | 0.026 | 1.7 | 2.7 |
| D3 | $4p^2$ | 0.00055 | 0.14 | 0.35 | 0.078 | 5.1 | 8.1 |
| total trimer | $150p^3$ | $2.4 \times 10^{-5}$ | 0.096 | 0.39 | 0.0034 | 3.6 | 9.0 |
| T1 | $18p^3$ | $2.9 \times 10^{-6}$ | 0.012 | 0.047 | 0.00041 | 0.43 | 1.1 |
| T2 | $36p^3$ | $5.8 \times 10^{-6}$ | 0.023 | 0.093 | 0.00082 | 0.85 | 2.2 |
| T3 | $24p^3$ | $3.8 \times 10^{-6}$ | 0.015 | 0.062 | 0.00055 | 0.57 | 1.4 |
| T4 | $72p^3$ | $1.2 \times 10^{-5}$ | 0.046 | 0.19 | 0.0016 | 1.7 | 4.3 |

[a] Refer to the notation used in Charts 2 and 3. [b] Relative to the mol % of the monomer.

**CHART 1: Example of a Geometrical Isomer of a [Ag(CN)$_2$−]$_2$ Dimer in the Cubic KCl Lattice[a]**

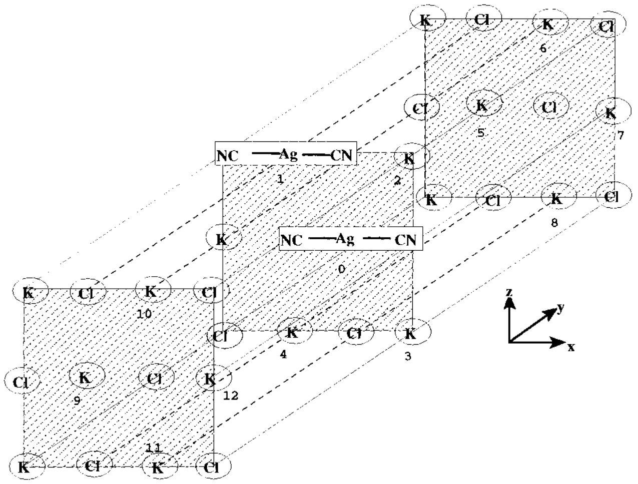

[a] The *y* scale is exaggerated for clarity.

(D1, D2, D3) in a KCl lattice as shown in Chart 2. The dimer in Chart 1, therefore, is the D3 isomer. A given [Ag(CN)$_2^-$] ion (site 0 in Chart 1) is surrounded by a total of 12 nearest-neighbor cation sites (sites 1−12). The linear ion at site 0 can be oriented along the *x*, *y*, or *z* axis. The probability is ($p$/3) for each of these three orientations. The ion at site 0 is oriented along the *x* axis in Chart 1. The probability for this ion is, therefore, ($p$/3). There are three sets of equivalent sites for the nearest-neighbor ion to the ion at site 0: (1−4), (5, 7, 9, 12), and (6, 8, 10, 11). Orientation of the [Ag(CN)$_2^-$] ion in each of these sites results in dimers with geometries and statistical probabilities as shown in Table 4. It is noted that not all orientations are necessarily possible for the nearest-neighbor ions. For example, the [Ag(CN)$_2^-$] ion at site 1 can be oriented only along the *x* or *y* axis but not the *z* axis if the ion at site 0 is oriented along the *x* axis. Orientations along the *x* and *y* axes give isomers D3 and D2, respectively, with a probability of ($p$/2) for each. Therefore, the probability for the D3 dimer shown in Chart 1 is ($p$/3)($p$/2), or ($p^2$/6). Compilation of the data in Table 4 for each [Ag(CN)$_2^-$]$_2$ isomer gives the overall results in Table 3.

The [Ag(CN)$_2^-$]$_3$ trimer has over 25 isomers in KCl if one considers the CN$^-$ ligands. These trimer isomers can be subdivided into four structures (T1, T2, T3, T4), based on the distribution of only the Ag$^+$ ions in KCl. Chart 3 shows the structure of each isomer. The total probability for each isomer is shown in Table 3. It should be pointed out that although the CN$^-$ ions are ignored in the categorization of the trimer structures, they are accounted for in the calculations. Ignoring the CN$^-$ ions in the distribution calculations of the [Ag(CN)$_2^-$]$_3$ trimers gives erroneous results because not all orientations are possible (as demonstrated in the above description of the dimer calculations).

It is noted that the statistical probability of the doped trimers: dimers:monomers increases as the Ag content increases in single crystals of KCl. This increase agrees qualitatively with the luminescence results shown in Figure 2. We have shown in ref 30 that quantitative trends cannot be obtained from the statistical analysis because thermodynamic factors must be considered. Given the favorable tendency for the aggregation of [Ag(CN)$_2^-$] units as we established earlier based on MO calculations,[28−30] the statistical ratio of the longer [Ag(CN)$_2^-$]$_n$ oligomers is largely underestimated by the statistical analysis.

According to Table 3, the total statistical probability is lower for the trimers than the dimers in all three doped crystals, including the P3 crystal that has the highest Ag content. This observation is in agreement with the infrared spectra. Note that the lower-frequency peaks are the most dominant in the infrared spectra of all the crystals studied (Figure 1). The low doping levels of [Ag(CN)$_2^-$] in the host lattices also suggest that the likelihood is greater for finding more isolated-ion sites than oligomer sites. If direct excitation of [Ag(CN)$_2^-$]$_n$ species is the only mechanism responsible for the individual luminescence bands of the [Ag(CN)$_2^-$]/KCl system, the intensity of band C should still be much lower than the intensity of band A, even in the crystal that contains the highest Ag content. This is because both the statistical analysis and the infrared spectra

**CHART 2: Structures of the Three Possible Geometrical Isomers of a $[Ag(CN)_2^-]_2$ Dimer in KCl[a]**

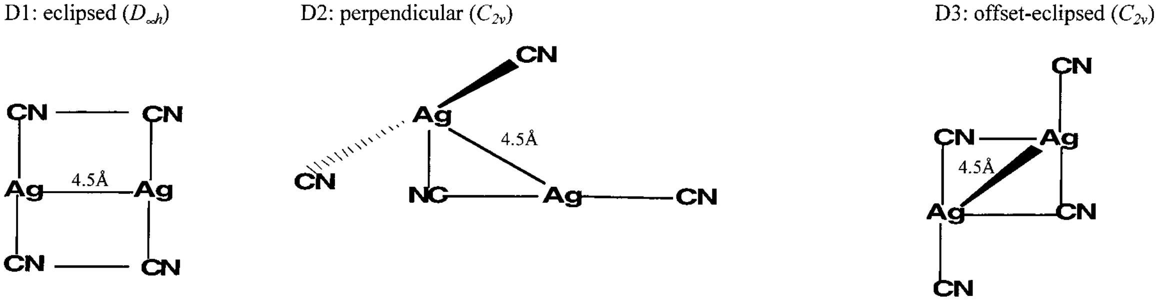
D1: eclipsed ($D_{\infty h}$) D2: perpendicular ($C_{2v}$) D3: offset-eclipsed ($C_{2v}$)

[a] In terms of the numbering used in Chart 1, the D1, D2, and D3 isomers can be obtained if adjacent $[Ag(CN)_2^-]$ linear ions at sites (0,1) are oriented along (*y*,*y*), (*y*,*x*), and (*x*,*y*), respectively. The orientation shown in Chart 1 corresponds to D3.

**CHART 3: Structures of the Four Possible Orientations of Ag Atoms of a $[Ag(CN)_2^-]_3$ Trimer in KCl[a]**

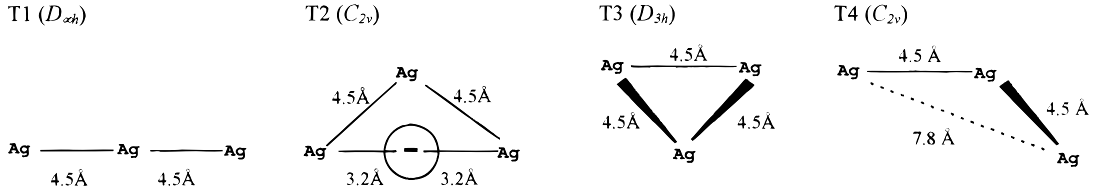
T1 ($D_{\infty h}$) T2 ($C_{2v}$) T3 ($D_{3h}$) T4 ($C_{2v}$)

[a] In terms of the numbering used in Chart 1, the T1, T2, T3, and T4 isomers can be obtained if Ag atoms in the trimer are at sites (1,0,3), (1,0,2), (1,0,9), and (1,0,12), respectively. The circle in T2 represents an anionic site, which may be occupied by $Cl^-$ or $CN^-$.

**TABLE 4: Outline of the Method Used for the Calculation of the Statistical Distribution Analysis of the Geometrical Isomers of the $[Ag(CN)_2^-]_2$ Dimer**

| | sites 1−4 | | | sites 5, 7, 9, 12 | | | sites 6, 8, 10, 11 | | |
|---|---|---|---|---|---|---|---|---|---|
| site 0 | *x* | *y* | *z* | *x* | *y* | *z* | *x* | *y* | *z* |
| *x*<br>(*p*/3) | D3<br>(*p*/2) | D2<br>(*p*/2) | 0 | D3<br>(*p*/2) | 0 | D2<br>(*p*/2) | D1<br>(*p*/3) | D2<br>(*p*/3) | D2<br>(*p*/3) |
| *y*<br>(*p*/3) | D2<br>(*p*/3) | D1<br>(*p*/3) | D2<br>(*p*/3) | 0 | D3<br>(*p*/2) | D2<br>(*p*/2) | D2<br>(*p*/2) | D3<br>(*p*/2) | 0 |
| *z*<br>(*p*/3) | 0 | D2<br>(*p*/2) | D3<br>(*p*/2) | D2<br>(*p*/3) | D2<br>(*p*/3) | D1<br>(*p*/3) | D2<br>(*p*/2) | 0 | D3<br>(*p*/2) |

[a] The site numbers (0−12) are according to the numbering used in Chart 1. [b] Refer to the notation used in Chart 2 for the geometrical isomers (D1−D3) of $[Ag(CN)_2^-]_2$. The probability for each isomer is shown in parentheses.

suggest that the trimer population is less than the dimer population in all crystals studied. The kinetic model proposed in a later section suggests that besides direct excitation, energy-transfer pathways are responsible for the luminescence of the $[Ag(CN)_2^-]$/KCl crystals. The statistical analysis is discussed in relation to this kinetic model in the Concluding Remarks section.

**Time-Resolved Photoluminescence Spectra.** The corrected excitation spectra of the different luminescence bands for the $[Ag(CN)_2^-]$/KCl system are shown in Figure 3. One should note that the excitation spectra intersect near 250 and 270 nm. The importance of these points lies in the fact that one can excite at these wavelengths and see more than one emission. Therefore, time-resolved measurements can be used to study possible energy-transfer pathways between the excitons characteristic of the different $[Ag(CN)_2^-]_n$ oligomers.

Time-resolved measurements for the $[Ag(CN)_2^-]$/KCl single crystal with 2.7% Ag (P2) are shown in Figure 4. The excitation wavelength was selected as 250 nm in order to show energy transfer from dimer sites (band A) to trimer sites (band C). Figure 4 illustrates that the intensity ratio of band C/band A increases when either the delay time of the laser pulse is increased (Figure 4a) or the gate width is increased (Figure 4b). This is a nice illustration of energy transfer between band A excitons (characteristic of $[Ag(CN)_2^-]_2$ dimer sites) to band C excitons (characteristic of $[Ag(CN)_2^-]_3$ linear trimer sites).

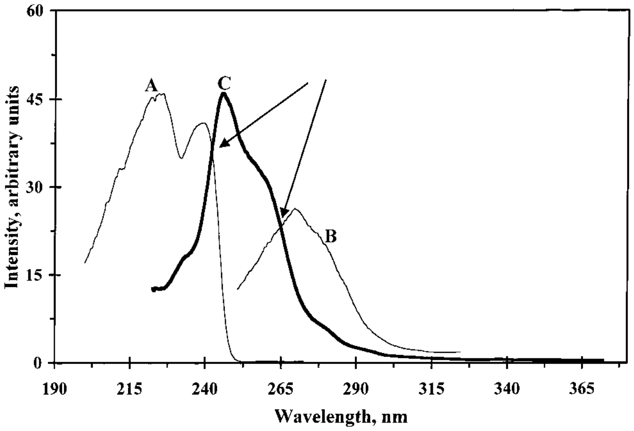

**Figure 3.** Corrected excitation spectra of a $[Ag(CN)_2^-]$/KCl single crystal at 77 K monitoring emissions that correspond to bands A, B, and C. The arrows at ~250 and ~270 nm represent intersection points between bands A and C and between bands B and C, respectively. These wavelengths were used in the time-resolved spectra.

Similar results have been obtained regarding energy transfer between excitons characteristic of different isomers of $[Ag(CN)_2^-]_3$ doped trimers. Note in Table 2 three different bands have been assigned for the $[Ag(CN)_2^-]_3$ species. An inspection of the excitation spectra (Figure 3) reveals that if one selects an excitation wavelength near 270 nm, the trimer bands B and C are observed. We have carried out time-resolved measurements for a $[Ag(CN)_2^-]$/KCl single crystal using 270 nm (Figure 5). When the delay time of the laser pulse is increased from 0 to 10 $\mu$s, the intensity ratio of band B-2/band B-1 increases. A further increase in the delay time from 10 to 20 to 30 to 40 $\mu$s results in an increase in the intensity ratio of band C/band B-2. Therefore, the time-resolved spectra in Figure 5 provide a nice illustration of the energy transfer between $*[Ag(CN)_2^-]_3$ excitons that represent bands B-1, B-2, and C.

**Electronic Structure Calculations.** In exciplex tuning by varying the dopant concentration, the energy-transfer processes

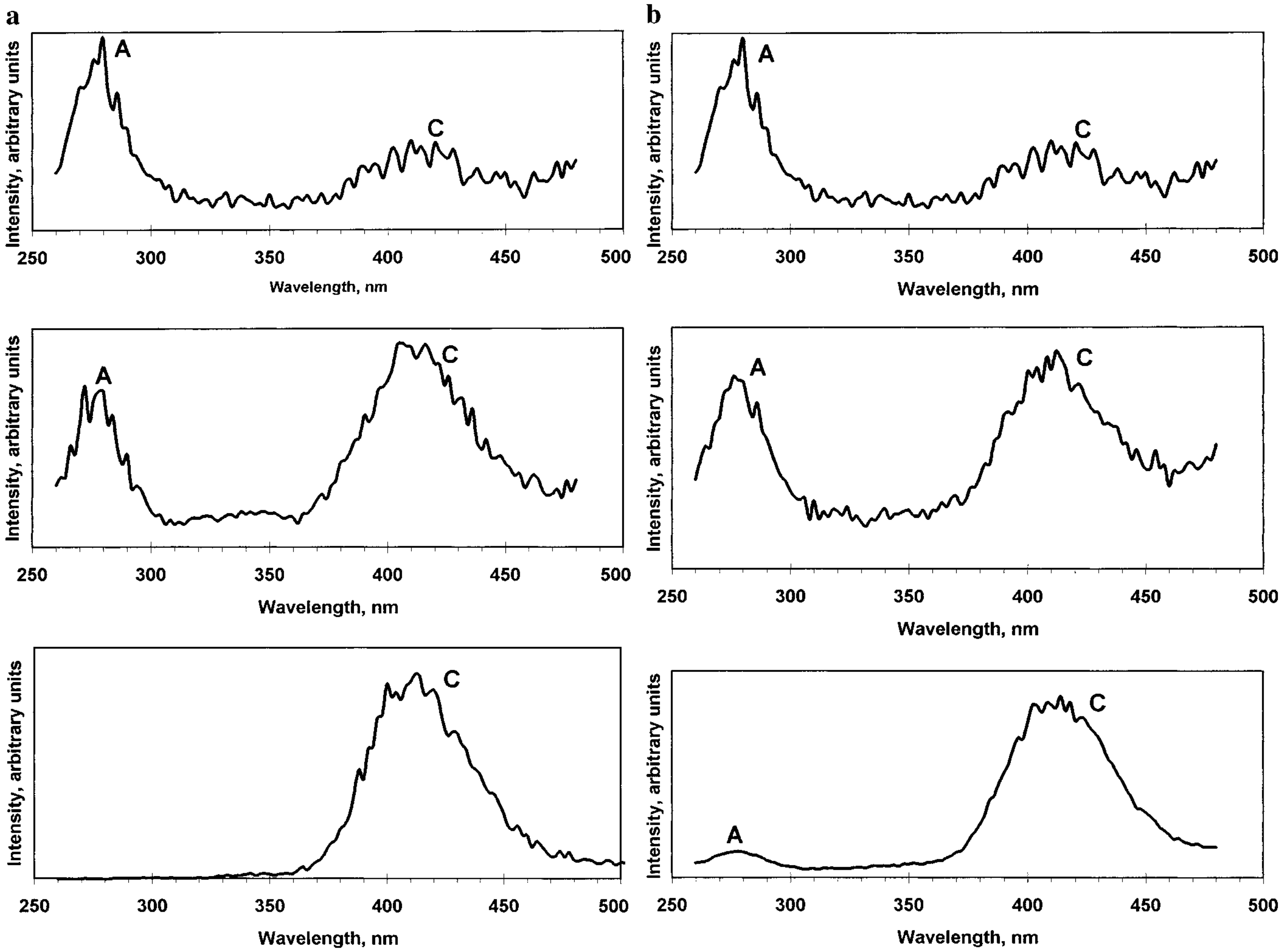

**Figure 4.** Time-resolved measurements for the [Ag(CN)$_2^-$]/KCl single crystal with 2.7% Ag (P2). The excitation wavelength was selected as 250 nm in order to show energy transfer from dimer sites (band A) to trimer sites (band C). The spectra were obtained with (delay time, gate) pairs as follows: (a) top-to-bottom (0, 5), (5, 5), and (20, 200) $\mu$s; (b) top-to-bottom (0, 5), (0, 10), and (0, 200) $\mu$s.

between [Ag(CN)$_2^-$]$_n$ sites seem to proceed more favorably in the direction of the lower-energy bands. To provide a theoretical model that accounts for the complicated energy-transfer pathways in the [Ag(CN)$_2^-$]/KCl system, we have carried out a series of molecular orbital calculations. Extended Hückel calculations have been carried out for models that represent the different luminescent oligomers in the [Ag(CN)$_2^-$]/KCl system. The calculations have been carried out for both the ground state and the first excited state of these oligomers in order to relate the results of the calculations to the experimental data. Figure 6 provides a schematic diagram that summarizes the results of these calculations. Different optical transitions and energy-transfer pathways are illustrated in Figure 6. The emissions denoted A, B-1, B-2, and C follow the notation in Table 2. The model in Figure 6 relates the observed luminescence results to the results of these theoretical calculations.

The energy-transfer processes in the crystals studied are, in essence, multistep quenching pathways. The formation of stable excimers quenches any luminescence from isolated ions and results in the observation of band A. Moreover, as the concentration of [Ag(CN)$_2^-$] increases in KCl, the excimer emission is quenched because of the formation of more stable *[Ag(CN)$_2^-$]$_n$ exciplexes, and thus, band A is quenched and a lower-energy emission (band C) becomes more dominant (Figure 2). This is a very similar situation to the trends observed in the luminescence behavior of solutions of excimer-forming organic compounds such as pyrene.[39] In inorganic compounds, exciplex formation has often been indicated by the quenching of the luminescence of the fluorophores (or phosphorophores) upon the addition of other species with which the exciplexes form. A new low-energy emission appears if the formed exciplex is luminescent. The metal−metal bonded exciplexes reported by Nagle et al. are luminescent, and thus they illustrate this behavior.[40] On the other hand, if the formed exciplexes are not luminescent, then exciplex formation is merely indicated by the quenching of the luminescence of the original fluorophore without the appearance of another emission for the exciplex. There are many examples to illustrate this behavior such as the exciplexes formed between porphyrins and transition-metal ions.[41,42] The luminescence behavior in the study herein is more complicated than that in all these other studies. The pattern of the quenching of one band and the appearance of a lower-energy band occurs in multiple steps in [Ag(CN)$_2^-$]/KCl crystals, as opposed to the one-step patterns observed in all organic and other inorganic exciplex systems. Moreover, the luminescence behavior in Figure 2 illustrates a new case in which both the quenched emission and the new emission are characteristic of excimers and exciplexes, whereas in the other studies only the new emission is an excimer or exciplex emission.

**Kinetics of Energy Transfer in [Ag(CN)$_2^-$]/KCl Doped Crystals.** For the kinetic treatment of energy transfer in the [Ag(CN)$_2^-$]/KCl system, we consider each luminescent [Ag(CN)$_2^-$]$_n$ oligomer in the single crystal as a separate species. Upon the excitation with a wavelength characteristic of a given [Ag(CN)$_2^-$]$_n$

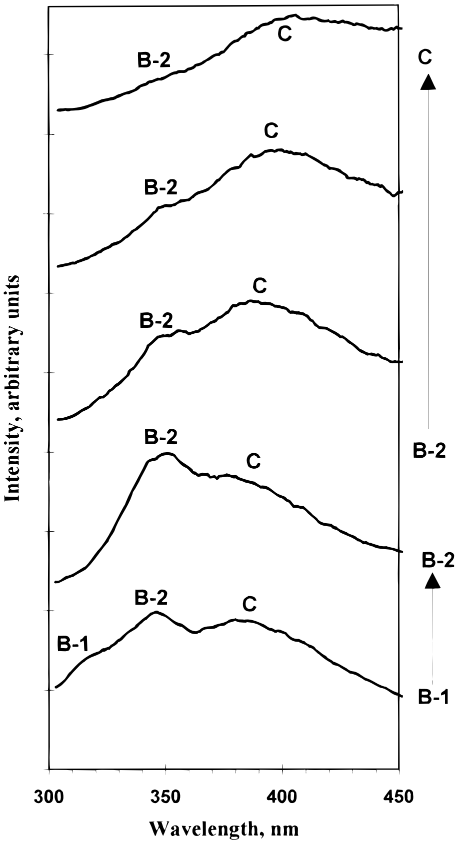

**Figure 5.** Time-resolved measurements for a [Ag(CN)$_2^-$]/KCl single crystal. The excitation wavelength was selected as 270 nm in order to show energy transfer between different trimer sites (bands B-1, B-2, and C). The delay time after the laser pulse was (bottom-to-top): 0, 10, 20, 30, and 40 $\mu$s, respectively. The gate width was 10 $\mu$s in all spectra.

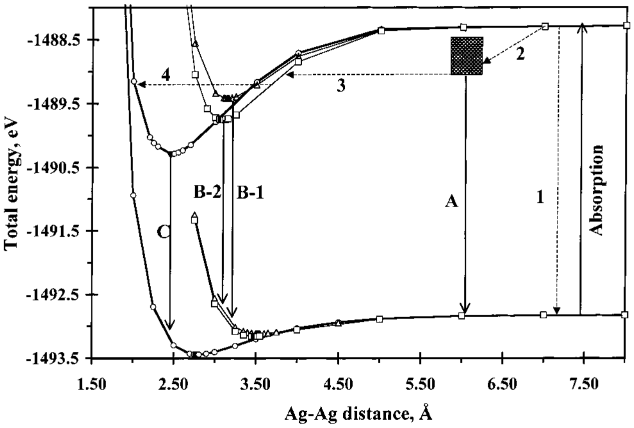

**Figure 6.** Model for energy transfer between different [Ag(CN)$_2^-$]$_n$ clusters based on extended Hückel molecular orbital calculations. The potential surfaces represent ground and first excited states of three different isomers of [Ag(CN)$_2^-$]$_3$ trimers. The dimer excited state is represented by a band in order to fit the data on the same scale. The emissions denoted A, B-1, B-2, and C follow the notation in Table 2. The numbers denoting the nonradiative transitions are as follows: 1, nonradiative de-excitation of the monomer excited state to the ground state; 2, nonradiative relaxation of the monomer excited state to the *[Ag(CN)$_2^-$]$_2$ excimer state; 3, dimer-to-trimer energy transfer; 4, energy transfer between different trimer isomers.

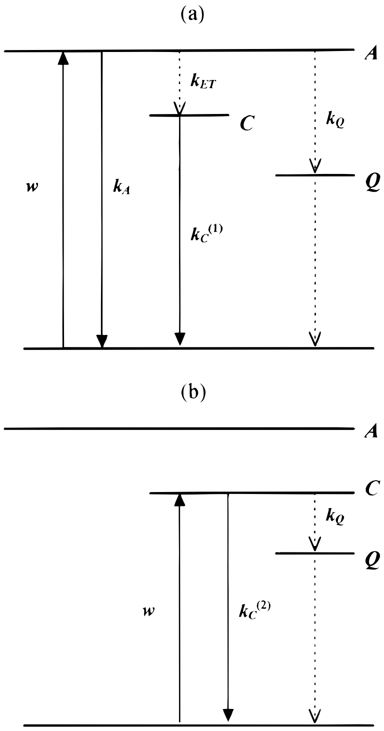

**Figure 7.** Kinetic models for energy-transfer processes present in single crystals of [Ag(CN)$_2^-$]/KCl. The two mechanisms represent energy transfer from excitons characteristic of band A to band C excitons (a) and direct excitation of band C excitons (b), respectively. Solid and dashed lines represent radiative and nonradiative processes, respectively.

oligomer, this oligomer can either emit light or transfer its excitation energy to another oligomer. As an example, Figure 7 shows the kinetics of the various radiative and nonradiative processes in the [Ag(CN)$_2^-$]/KCl doped crystal labeled as P2 herein. According to this simplified model, excitation occurs to the [Ag(CN)$_2^-$]$_n$ oligomer that is responsible for band A, at a rate equals to "$w$". The excited species can decay either radiatively by emitting band A ($k_A$) or nonradiatively. The nonradiative processes can be either energy transfer to the sites responsible for band C ($k_{ET}$), or multiphonon relaxation to unintentional crystal defects that act as quenching traps ($Q$). The former process leads to the emission of band C ($k_C^{(1)}$), while the latter process leads to quenching of the dicyanoargentate(I) luminescence.

The emissions from the sites responsible for bands A and C have time dependencies that can be described as follows according to the model shown in Figure 7a:

$$dN_A/dt = w - k_A N_A - k_{ET} N_A - k_Q N_A \qquad (1)$$

$$dN_C^{(1)}/dt = k_{ET} N_A - k_C^{(1)} N_C \qquad (2)$$

where $N_A$ and $N_C^{(1)}$ represent the population of the excitons characteristic of bands A and C, respectively. The solutions of the ordinary differential eqs 1 and 2 for a $\delta$-pulsed excitation by considering the initial condition $N_C = 0$ are:

$$N_A(t) = N_A(0) \exp(-\{k_A + k_{ET} + k_Q\}t) \qquad (3)$$

$$N_C(t)^{(1)} = [k_{ET}/(k_C^{(1)} - k_A - k_{ET} - k_Q)] \times [\exp(-\{k_A + k_{ET} + k_Q\}t) - N_A(0) \exp(-k_C^{(1)} t)] \qquad (4)$$

According to eq 3, band A decays exponentially with only one lifetime component. The experimental values of the lifetimes of the luminescence bands obtained with $\lambda_{exc} = 250$ nm are summarized in Table 5. Band A has a single lifetime ($\tau_A = 2.8$ $\mu$s) according to Table 5. The mechanism depicted in Figure 7a, therefore, accurately describes the time dependence of band

**TABLE 5: Lifetime Data for the Luminescence Bands of the P2 Crystal of $[Ag(CN)_2^-]$/KCl at 77 K and Using 250-nm Excitation**

| emission band[a] | monitored $\lambda^{em}$ | lifetime, $\mu$s |
|---|---|---|
| A | 280 nm | $2.78 \pm 0.19$ |
| B | 345 nm | $6.48 \pm 0.88$ |
| C | 415 nm | $27.4 \pm 3.5$ (39%)<br>$64.4 \pm 1.8$ (61%) |

[a] Although band B was weak in this crystal, it was strong enough to obtain a reliable lifetime value. Band D was virtually nonexistant in this crystal.

A emission. On the other hand, eq 4 predicts that band C has a dual lifetime: a rise time due to the feeding mechanism from A and a decay time of $1/k_C^{(1)}$. The rise time component of the band C emission should be equal in magnitude to the decay time of band A, according to eq 4. Experimentally, band C has a virtual zero rise time and a dual lifetime decay with a slow component $\tau_C^{(1)} = 64$ $\mu$s and a fast component $\tau_C^{(2)} = 27$ $\mu$s. Therefore, the time dependence of the band C emission cannot be described by the model shown in Figure 7a alone.

The most likely interpretation of the dual emission for band C is that one of the two components in the band C emission is actually due to a direct excitation for band C. The excitation wavelength used for the lifetime data herein was 250 nm, the shortest wavelength we were able to use to give measurable luminescence intensity. At this wavelength, the clusters responsible for band C can be excited directly ($\lambda_{exc} = 250-270$ nm for band C, Table 2). The kinetic treatment for this situation is based on the mechanism shown in Figure 7b. According to this mechanism, the time dependence of the dicyanoargentate(I) emission is as follows:

$$dN_A^{(2)}/dt = 0 \tag{5}$$

$$dN_C^{(2)}/dt = w - k_C^{(2)}N_C - k_QN_C \tag{6}$$

For simplicity it is assumed that the rates of excitation ($w$) and quenching ($k_Q$) are the same in both mechanisms in Figure 7. The solution to the ordinary differential eq 6 for a $\delta$-pulsed excitation by considering the initial condition $N_A = 0$ is:

$$N_C(t)^{(2)} = N_C(0) \exp(-\{k_C^{(2)} + k_Q\}t) \tag{7}$$

According to eq 7, the band C emission by the direct excitation mechanism (Figure 7b) decays exponentially with $\tau_C^{(2)} = 1/k_C^{(2)}$.

The overall emission due to band C is now described by a combination of eqs 4 and 7. It is reasonable to assume that the excitation rate ($w$) is much faster than the feeding rate ($k_{ET}$). This implies that the slow component of the band C decay lifetime (64 $\mu$s) is due to energy transfer from A while the fast component (27 $\mu$s) is due to direct excitation. The experimental lifetime results can now be explained in terms of the kinetic model shown in Figure 7. For band A, only the mechanism shown in Figure 7a applies, and this gives rise to a single lifetime decay (eq 3), in agreement with the experimental results ($\tau_A = 2.8$ $\mu$s). The time dependence for band C emission is more complicated. In the short time domain, band C emission exhibits a rise time due to the feeding mechanism from band A and a decay time due to direct excitation. According to the experimental results, the fast component of the decay time for band C is 27 $\mu$s, significantly longer than the decay time of band A (2.8 $\mu$s). Therefore, the rate-determining step in the short-time domain for band C is direct excitation (Figure 7b). In the long-time domain, the feeding mechanism from band A (Figure 7a) is solely responsible for the time dependence for the band C emission, and this gives rise to the slow component in the decay time for band C (64 $\mu$s). The time-resolved spectra provide a nice illustration of the aforementioned kinetic model. The increase in the relative intensity of band C, with time, accompanied by the reduction of the relative intensity of band A, is unmistakable in the time-resolved spectra obtained for the P2 crystal upon exciting with 250 nm (see the above discussion of Figure 4). Therefore, we conclude that the kinetic model shown in Figure 7 explains the experimental lifetime and time-resolved data.

An examination of the luminescence emission and excitation spectra supports the conclusion of the kinetic model that both direct excitation and energy transfer are responsible for the $[Ag(CN)_2^-]$/KCl luminescence bands. The direct excitation is indicated by the presence of intersection points in the excitation spectra, as discussed above. Energy transfer is confirmed by the strong spectral overlap between the emission of band A with the excitation of band C. It is well-known that for efficient energy transfer to occur, a strong spectral overlap must exist between the "donor emission" and the "acceptor absorption".[43] We regard the oligomer responsible for band A, $[Ag(CN)_2^-]_2$, as the donor while the oligomer responsible for band C, linear $[Ag(CN)_2^-]_3$, as the acceptor. Note that band A emission (or the "donor emission") starts at ~270 nm and extends to ~350 nm (Figure 2). Meanwhile, band C excitation (or the "acceptor absorption") is exhibited at wavelengths shorter than 315 nm (Figure 3). An overlap between the $[Ag(CN)_2^-]_2$ donor emission and the $[Ag(CN)_2^-]_3$ acceptor absorption exists in the wavelength range of 270−315 nm. That is, the donor−acceptor spectral overlap occurs over a range of nearly $5.3 \times 10^3$ cm$^{-1}$.

Normally, the "donor" and "acceptor" are different chemical species in energy-transfer processes. For example, the donor may be a transition-metal complex[44] or a protein molecule,[7] while the acceptor in both cases is a rare earth ion. The energy transfer suggested to exist herein is unusual because it occurs between the same type of species, $[Ag(CN)_2^-]_n$, but the donor and acceptor differ in the oligomer length "$n$" or conformation. That is, different $[Ag(CN)_2^-]_n$ oligomers act as independent species in the energy-transfer processes suggested herein in the $[Ag(CN)_2^-]$/KCl system. The observation of different physical behavior between the same type of species in the same lattice, although quite unusual, is not unprecedented. An example of this behavior is $Ag_5SiO_4$, whose structure and physical properties suggest that $[Ag_6]^{4+}(Ag^+)_4(SiO_4^{4-})_2$ is a more reasonable formulation than the empirical formula of the compound.[45] The fact that one $[Ag(CN)_2^-]_n$ species acts as a donor while another as an acceptor for energy transfer in the $[Ag(CN)_2^-]$/KCl systems provides the first illustration that the difference among sublattices of the same silver-based material can be in the form of independent luminescence behavior for each sublattice.

## Concluding Remarks

The study herein provides an illustration of the rich luminescence behavior of dicyanoargentates(I). Multiple luminescence bands are present in $[Ag(CN)_2^-]$/KCl doped crystals. The study herein suggests that the luminescence of the $[Ag(CN)_2^-]$/KCl system can be *tuned* by changing the dopant concentration. In ref 30 we have described the tunability of the dicyanoargentates(I) luminescence by changing the excitation wavelength. Individual $[Ag(CN)_2^-]_n$ oligomers are responsible for the individual luminescence bands in $[Ag(CN)_2^-]$/KCl. This adds to the multiple experimental evidence in the literature that Ag(I) species in one material can exist in multiple cluster sites that have independent physical and chemical behavior.[6,42] The independent photophysical behavior of different $[Ag(CN)_2^-]_n$ oligomers within the KCl host is illustrated by the appearance of an individual band for each oligomer. Time-resolved spectra suggest the presence of energy transfer from the $[Ag(CN)_2^-]_n$ oligomers responsible for the higher-energy bands to the oligomers responsible for the lower-energy bands.

The kinetic analysis suggests that excitation of a given $[Ag(CN)_2^-]_n$ oligomer can lead either to luminescence from the same oligomer or to the transfer of the excitation energy to a different oligomer. As the silver concentration increases in $[Ag(CN)_2^-]$/KCl crystals, the statistical probability of the population of $[Ag(CN)_2^-]_3$ trimers increases relative to the population of the corresponding dimers and monomers. This leads to an increase in the relative intensity of the luminescence bands characteristic of the trimer, as observed experimentally. This result can be explained by the proposed kinetic model as follows. (1) An increase in the trimer population leads to an increase in the number of photons emitted by a direct excitation of the $[Ag(CN)_2^-]_3$ ions. (2) An increase in the trimer population in the concentrated crystals means that the number of acceptors of the excitation energy from $^*[Ag(CN)_2^-]_2$ excitons increases. The driving force of this energy-transfer process is the lower energy of $^*[Ag(CN)_2^-]_3$ exciplexes than the energy of the $^*[Ag(CN)_2^-]_2$ excimers, as suggested by our MO calculations. Both (1) and (2) lead to an increase in the relative intensity of the lower-energy bands in $[Ag(CN)_2^-]$/KCl because the bands characteristic of $[Ag(CN)_2^-]_3$ have lower energies than the energies of the corresponding $[Ag(CN)_2^-]_2$ bands.

**Acknowledgment.** We thank the Donors of the Petroleum Research Fund, administered by the American Chemical Society, for the support of this research. D.R.H. acknowledges a Robert A. Welch Foundation undergraduate research scholarship at Angelo State University.

## References and Notes

(1) (a) Zhanpeisov, N. U.; Nakatsuji, H.; Hada, M.; Nakai, H.; Anpo, M. *Catal. Lett.* **1996**, *42*, 173. (b) Beutel, T.; Adelman, B. J.; Lei, G.-D.; Sachtler, W. M. H. *Catal. Lett.* **1995**, *32*, 83. (c) Negishi, N.; Matsuoka, M.; Yamashita, H.; Anpo, M. *J. Chem. Phys.* **1993**, *97*, 5211.

(2) (a) Exstrom, C. L.; Sowa, J. R., Jr.; Daws, C. A.; Janzen, D.; Mann, K. R. *Chem. Mater.* **1995**, *7*, 15. (b) Daws, C. A.; Exstrom, C. L.; Sowa, J. R., Jr.; Mann, K. R. *Chem. Mater.* **1997**, *9*, 363.

(3) (a) Liska, P.; Vlachopoulos, N.; Nazeeruddin, M. K.; Comte, P.; Grätzel, M. *J. Am. Chem. Soc.* **1988**, *110*, 3686. (b) Nazeeruddin, M. K.; Kay, A.; Rodicio, I.; Baker, R. H.; Müller, E.; Liska, P.; Vlachopoulos, N.; Grätzel, M. *J. Am. Chem. Soc.* **1993**, *115*, 6382. (c) Kohle, O.; Ruile, S.; Grätzel, M. *Inorg. Chem.* **1996**, *35*, 4779. (d) Nazeeruddin, M. K.; Müller, E.; Baker, R. H.; Vlachopoulos, N.; Grätzel, M. *J. Chem. Soc., Dalton Trans.* **1997**, 4571.

(4) Cheng, L. T.; Tam, W.; Eaton, D. F. *Organometallics* **1990**, *9*, 2856.

(5) Prasad, P. N.; Reinhardt, B. A. *Chem. Mater.* **1990**, *2*, 660.

(6) Jansen, M. *Angew Chem.* **1987**, *99*, 1136; *Angew. Chem., Int. Ed. Engl.* **1987**, *26*, 1098.

(7) (a) Horrocks, W. DeW., Jr.; Sudnick, D. R. *Acc. Chem. Res.* **1981**, *14*, 384. (b) Richardson, F. S. *Chem. Rev.* **1982**, *82*, 541. (c) Friedman, A. E.; Chambron, J. C.; Sauvage, J. P.; Turro, N. J.; Barton, J. K. *J. Am. Chem. Soc.* **1990**, *112*, 4960.

(8) Edel, A.; Marnot, P. A.; Sauvage, J. P. *Nouv. J. Chim.* **1984**, *8*, 495.

(9) Kruglik, G. S.; Skripko, G. A.; Shkadarevich, A. P.; Ermolenko, N. N.; Gorodetskaya, O. G.; Belokon, M. V.; Shagov, A. A.; Zolotareva, L. E. *Opt. Spectrosc. (USSR)* **1985**, *59*, 439.

(10) Moine, B.; Pedrini, C.; Duloisy, E.; Boutinaud, P.; Parent, C.; Le Flem, G. *J. Phys. IV* **1991**, *C7*, 289.

(11) Blonder, R.; Levi, S.; Tao, G.; Ben-Dov, I.; Willner, I. *J. Am. Chem. Soc.* **1997**, *119*, 10467.

(12) Wolf, M. O.; Fox, M. A. *J. Am. Chem. Soc.* **1995**, *117*, 1845.

(13) Mansour, M. A.; Connick, W. B.; Lachicotte, R. J.; Gysling, H. J.; Eisenberg, R. *J. Am. Chem. Soc.* **1998**, *120*, 1329.

(14) Von der Austin, W.; Stolz, H. *J. Phys. Chem. Solids* **1990**, *51*, 765.

(15) Hamilton, J. F. *Adv. Phys.* **1988**, *37*, 359.

(16) Ueta, M.; Kanzaki, H.; Kabayashi, K.; Toyozawa, Y.; Hanamura, E. *Excitonic Processes in Solids*; Springer: Berlin, 1986; pp 309−69.

(17) (a) Moser, F.; Barkay, N.; Levite, A.; Margalit, E.; Paiss, I.; Sa'ar, A.; Schnitzer, I.; Zur, A.; Katzir, A. *Proc. SPIE* **1990**, *1228*, 128. (b) Baetzold, R. C. *J. Phys. Chem. B* **1997**, *101*, 8180.

(18) Pedrini, C.; Jacquier, B. *Phys. Lett. A* **1979**, *69*, 457. Pedrini, C.; Chermette, H.; Gaume-Mahn, F. *J. Lumin.* **1981**, *24/25*, 213. Pedrini, C.; *Solid State Commun.* **1981**, *38*, 1237.

(19) Meijerink, A.; van Heek, M. M. E.; Blasse, G. *J. Phys. Chem. Solids* **1993**, *54*, 901.

(20) Mesnaoui, M.; Maazaz, M.; Parent, C.; Tanguy, B.; LeFlem, G. *Eur. J. Solid State Inorg. Chem.* **1992**, *29*, 1001.

(21) Köhler, B. U.; Weppner, W.; Jansen, M. *J. Solid State Chem.* **1985**, *57*, 227.

(22) Gruber, H.; Hess, H.; Popitsch, A.; Fischer, A. P. *J. Electrochem. Soc.* **1982**, *129*, 369.

(23) Popitsch, A. *J. Crystallogr. Spectrosc. Res.* **1985**, *15*, 603.

(24) Fortin, D.; Drouin, M.; Turcotte, M.; Harvey, P. D. *J. Am. Chem. Soc.* **1997**, *119*, 531.

(25) Vogler, A.; Kunkely, H. *Chem. Phys. Lett.* **1989**, *158*, 74.

(26) Henary, M.; Zink, J. I. *Inorg. Chem.* **1991**, *30*, 3111.

(27) Sabin, F.; Ryu, C. K.; Ford, P. C.; Vogler, A. *Inorg. Chem.* **1992**, *31*, 1941.

(28) Omary, M. A.; Webb, T. R.; Assefa, Z.; Shankle, G. E.; Patterson, H. H. *Inorg. Chem.* **1998**, *37*, 1380.

(29) Omary, M. A.; Patterson, H. H. *Inorg. Chem.* **1998**, *37*, 1060.

(30) Omary, M. A.; Patterson, H. H. *J. Am. Chem. Soc.* **1998**, *120*, 7696.

(31) (a) Yersin, H.; Gliemann, G. *Ann. N. Y. Acad. Sci.* **1978**, *313*, 539. (b) Gliemann, G.; Yersin, H. *Struct. Bond.* **1985**, *62*, 87 and references therein.

(32) Cummings, S. D.; Eisenberg, R. *J. Am. Chem. Soc.* **1996**, *118*, 1949.

(33) Melhuish, W. H. *J. Opt. Soc. Am.* **1962**, *52*, 1256.

(34) Pyykkö, P.; Lohr, L. L. *Inorg. Chem.* **1981**, *20*, 1950.

(35) (a) Jones, L. H. *J. Chem. Phys.* **1957**, *26*, 1578. (b) Hildago, A.; Mathieu, J. P. *Compt. Rend.* **1959**, *249*, 233. (c) Bottger, G. L. *Spectrochim. Acta* **1968**, *24A*, 1821. (d) Chadwick; Frankiss, S. G. *J. Mol. Struct.* **1968**, *2*, 281.

(36) Omary, M. A. Ph.D. Thesis, Graduate School, University of Maine, 1997.

(37) (a) Hoard, J. L. *Z. Kristallogr.* **1933**, *84*, 231. (b) Staritzky, E. *Anal. Chem.* **1956**, *28*, 419.

(38) (a) Sharpe, A. G. *The Chemistry of Cyano Complexes of the Transition Metals*; Academic Press: London, 1976. (b) Sillen, L. G.; Martell, A. E. *Stability Constants of Metal-Ion Complexes*; The Chemical Society: London, 1964; Special Publication 17.

(39) (a) Lowry, T. H.; Schuller-Richardson, K. *Mechanism and Theory in Organic Chemistry*; Harper&Row: New York, 1981; pp 919−925. (b) Turro, N. J. *Modern Molecular Photochemistry*; Benjamin/Cummings: Melano Park, CA, 1978; pp135−146. (c) Lamola, A. A. In *Energy Transfer and Organic Photochemistry*; Lamola, A. A., Turro, N. J., Eds.; Wiley-Interscience: New York, 1969; pp 54−60. (d) *The Exciplex*; Gordon, M., Ware, W. R., Eds.; Academic Press: New York, 1975. (e) Kopecky, J. *Organic Photochemistry: A Visual Approach*; VCH: New York, 1991; pp 38−40. (f) Michl, J.; Bonacic-Koutecky, V. *Electronic Aspects of Organic Photochemistry*; Wiley: New York, 1990; pp 274−286.

(40) (a) Clodfelter, S. A.; Doede, T. M.; Brennan, B. A.; Nagle, J. K.; Bender, D. P.; Turner, W. A.; LaPunzia, P. M. *J. Am. Chem. Soc.* **1994**, *116*, 11379. (b) Nagle, J. K.; Brennan, B. A. *J. Am. Chem. Soc.* **1988**, *110*, 5931.

(41) (a) Roy, J. K.; Whitten, D. G. *J. Am. Chem. Soc.* **1971**, *93*, 7093. (b) Roy, J. K.; Whitten, D. G. *J. Am. Chem. Soc.* **1972**, *94*, 7162. (c) Roy, J. K.; Carroll, F. A.; Whitten, D. G. *J. Am. Chem. Soc.* **1974**, *96*, 6349.

(42) (a) Kapinus, E. I.; Aleksankina, M. M.; Dilung, I. I. *J. Photochem.* **1982**, *21*, 125. (b) Kapinus, E. I.; Aleksankina, M. M.; Staryi, V. P.; Boghillo, V. I.; Dilung, I. I. *J. Chem. Soc., Faraday Trans. 2* **1985**, *81*, 631.

(43) Dexter, D. L. *J. Chem. Phys.* **1953**, *21*, 836.

(44) (a) Powell, R. C.; Blasse, G. *Struct. Bond.* **1980**, *42*, 43. (b) Kambli, U.; Güdel, H. U. *Inorg. Chem.* **1984**, *23*, 3479.

(45) Linke, C.; Jansen, M. *Inorg. Chem.* **1994**, *33*, 2614.